Rare Metal Materials and Engineering
Volume 47, Issue 12, December 2018
Online English edition of the Chinese language journal

Available online at www.sciencedirect.com

ScienceDirect

Cite this article as: Rare Metal Materials and Engineering, 2018, 47(12): 3678-3685.

ARTICLE

Improved Mechanical Properties of Additive Manufactured Ti-6Al-4V Alloy via Annealing in High Magnetic Field

Zhao Ruifeng[1], Li Jinshan[1], Zhang Ying[1], Li Peixuan[1], Wang Jiaxiang[1], Zou Chengxiong[1], Tang Bin[1], Kou Hongchao[1], Gan Bin[1], Zhang Liang[2,3], Wang Jun[1], William Yi Wang[1]

[1] State Key Laboratory of Solidification Processing, Northwestern Polytechnical University, Xi'an 710072, China; [2] Shanghai Engineering Research Center of 3D Printing Materials, Shanghai 200437, China; [3] Shanghai Research Institute of Materials, Shanghai 200437, China

Abstract: A novel magnetic-field-driving approach was proposed and used to efficiently enhance the mechanical properties of selective laser melting (SLM) Ti-6Al-4V. The microstructures of the as-built and the SLM specimens annealed at 400, 800 °C below the β transus, and 1200 °C above the β transus for 30 min in the high magnetic field of 7 T were comprehensively characterized in terms of X-ray diffraction, optical microscope, scanning electron microscope, and atomic force microscope. Lattice distortions induced by Al and V atoms were characterized by bonding charge density, providing an insight into the atomic and electronic basis for the solid solution strengthening mechanism and the martensitic transformation mechanism. Referring to the as-built specimens, the ultimate tensile strength and the elongation of annealed specimens at 400 and 1200 °C in 7 T high magnetic field increase due to the short annealing time. Based on the coupling effect of force field induced by the heat and magnetic, it is expected that the microstructures of SLM Ti-6Al-4V would be conventionally optimized through changing the phase transformation thermodynamics. The validation of this hypothesis will pave a path to develop a novel magnetic-field-driving approach efficiently enhancing the mechanical properties of additive manufactured materials.

Key words: Ti-6Al-4V; selective laser melting; heat treatment; bonding charge density

Ti-6Al-4V alloy, a kind of $\alpha+\beta$ dual-phase titanium alloys, is widely used in the aerospace, sporting products, medical device and petrochemical industries due to its high strength-to-weight ratio, good corrosion resistance and biocompatibility[1-5]. Recently, together with the significant improvement in computational tools and computational materials science, additive manufacturing (AM) approaches can fabricate geometrically complex or multifunctional components in near net shape form with rapid transfer of 3D designs to final components, paving a way to a new era of digital fabrication[6-11]. Selective laser melting (SLM) is a powder bed fusion AM approach suitable for fabricating smaller, complex geometries, with hollow unsupported passages/structures while directed energy deposition (DED) better suits larger parts with coarser features requiring higher deposition rates[5,12]. For instance, the SLM Ti-6Al-4V cellular structures with open-cell size of 100 μm have a high wear resistance, which is considerable for biomaterials[13]. Under extensive investigations of the AM Ti-6Al-4V[2,12-21], it is found that the SLM Ti-6Al-4V could be stronger than its wrought counterparts, but the ductility is noticeably below the required minimum threshold for critical structural applications, being a major remaining challenge to be addressed[5,16,19,21].

Since SLM is characterized by high temperature gradients and short interaction time, the build-up thermal stresses and the rapid solidification occur, which lead to segregation

Received date: October 25, 2018
Foundation items: National Natural Science Foundation of China (51690163); National Key Research and Development Program of China (2016YFB0701304, 2016YFB0701303); Project to Strengthen Industrial Development at the Grass-Roots Level (TC160A310/19); Shanghai Rising-star Program (18QB1400600)
Corresponding author: Li Jinshan, Ph. D., Professor, State Key Laboratory of Solidification Processing, Northwestern Polytechnical University, Xi'an 710072, P. R. China, E-mail: ljsh@nwpu.edu.cn

phenomena and the development of non-equilibrium phases[17,22]. The formation of martensitic phase reduces the ductility of AM Ti-6Al-4V[5]. For example, the lower toughness of the SLM Ti-6Al-4V than that of electron beam melting (EBM)-processed one is caused by the brittle fine acicular α' martensitic microstructure, which also has a low capacity to endure crack initiation and propagation[16,21,23]. It is believed that a small amount of intermetallic compound Ti_3Al could also precipitate in the local region rich in Al when the temperature reaches 500~600 °C[22]. In addition, both the SLM and the EBM Ti-6Al-4V present the mechanical anisotropy[1,21] and introduce the residual stress, which play a significant role in affecting the fatigue life and further applications[24-27]. Therefore, it is essential to reduce the residual stress and to optimize the microstructures of AM Ti-6Al-4V, which still call for more efforts to enhance the corresponding mechanical properties[1,5,12,28,29].

Although there are several well-defined standard heat treatments for Ti-6Al-4V, including the regular "mill anneal" (named treatment six) for cold deformed materials, the duplex anneal (named treatment seven), and the β anneal (named treatment eight)[17], the SLM Ti-6Al-4V should endure an unique heat treatment paradigm due to their different microstructures compared with those wrought ones[18]. As a result of reduced residual stress caused by the high temperature gradient and the rapid solidification during processing, the ductility of SLM Ti-6Al-4V can be improved through subsequent heat treatment or hot isostatic pressing (HIP) treatment[4,5,17,29].

It is understood that the heat treatment removes residual stresses and the HIP treatment reduces internal defects besides the microstructure optimizations[16,17,30]. The investigation of the microstructure evolution after different heat treatments was carried out to determine the microstructure in terms of applicability for the biomedical industry[26]. In particular, mechanical properties of the samples after stress relieving heat treatment at 650 °C for 3 h are complied with the international standard for Ti alloys for biomedical applications[15]. It is found that the post-SLM treatment at 850 °C for 2 h followed by furnace cooling enhances the ductility of SLM Ti-6Al-4V from (7.36±1.32)% of the as-built ones to (12.84±1.36)%[17]. Based on the β transus temperature, both the low-temperature and the high-temperature annealing strategies were investigated[18]. On the other hand, HIP treatment results in a lower maximum strength but higher ductility[29], which can also significantly improve the fatigue strength, by closing of the pores[4,31]. For example, while SLM Ti-6Al-4V specimens annealed at 800 °C for 2 h in argon atmosphere presented a similar fatigue life referring to conventionally processed one, the HIP treated ones at 920 °C for 2 h in argon atmosphere showed an enhanced fatigue life[32]. It also revealed that only a decrease in size of α-phase cluster could further improve the fatigue performance of SLM Ti-6Al-4V[32]. It is worth mentioning that post-SLM heat treatment is necessary, which affects the effectiveness of the AM process[16].

In the present work, a novel magnetic-field-driving approach was proposed and used to efficiently enhance the mechanical properties of SLM Ti-6Al-4V. Based on the coupling effect of force field induced by the heat and magnetic, it is expected that the microstructures of SLM Ti-6Al-4V would be conventionally optimized through changing the phase transformation thermodynamics, which is one type of novel phenomena observed in high magnetic field[33-35]. The validation of this hypothesis will pave a path to develop a novel magnetic-field- driving approach efficiently enhancing the mechanical properties of additive manufactured materials.

1 Experiment

The gas atomized Ti-6Al-4V spherical powder with a size of 15~50 μm was used as the raw material to fabricate the SLM samples via EOS M290 device in an argon protective atmosphere[3]. According to a series of preliminary tests, the screened suitable processing parameters were determined, including the scan speed of 1200 mm/s, the laser power of 280 W, the laser spot of 100 μm, the powder layer thickness of 30 μm and the hatch spacing 80 μm, yielding the SLM Ti-6Al-4V parts/specimens with a relative density as high as 98.3%[3]. The 12 mm×12 mm×56 mm rectangular blocks were fabricated via a zig-zag scanning strategy, which were cut into the tensile specimens along the scanning direction, as shown in Fig.1. In order to reduce the residual stress and to opimize the microstructures, these samples were annealed at 400, 800 °C below the β transus, and 1200 °C above the β transus for 30 min in the high magnetic field of 7 T and subsequently cooled in the air.

Under the guidance of the recommended national standard GB/T 3246.1-2000, those samples used for the microstructure characterizations were polished on SiC papers with a grid of 400#, 600#, 800#, 1200#, and 2000#, followed by Buehler

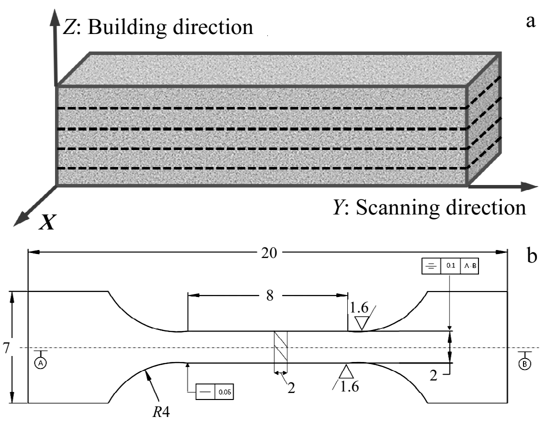

Fig.1 Schematic diagram of SLM-processed Ti-6Al-4V samples: (a) 12 mm×12 mm×56 mm blocks and (b) the tensile specimens along the scanning direction

diamond paste on polishing cloth. Subsequently, they were etched in an acid mixture consisting of HF, HNO_3 and distilled water at the volumetric ratio of 1:2:5. Finally, they were rinsed with absolute ethyl alcohol to remove the dust on the surface. The X-ray diffractometer with Cu Kα radiation (DX-2700), the optical microscope (OLYMPUS), scanning electron microscope (ZEISS GemniSEM500), and atomic force microscopy were used to analyze the microstructures comprehensively.

With the theoretical and experimental progress of material characterizations, the vivid atomic/molecule "Hollywood" would be constructed by atomic and electronic actors[36-43]. Bonding charge density ($\Delta\rho$)[38,40-43] was derived through the charge density difference between the one from the self-consistent calculation and the one from the non-self-consistent calculation, revealing the electronic redistributions constructing the chemical bond. Here, effects of Al and V on the $\Delta\rho$ of α and β Ti were calculated by first-principles calculations via the Vienna ab initio simulation package (VASP). The supercell with 96 atoms was applied in the calculations of α-Ti, β-Ti, α-$Ti_{95}X$, and β-$Ti_{95}X$. The corresponding setting parameters and the lattice distortion analysis are as same as those in our previous works of α-Ti and α-$Ti_{95}X$[37,42]. The visualization for electronic and structural analysis (VESTA) code[44] was used to generate the contour and isosurface plots of $\Delta\rho$.

2 Results and Discussion

2.1 Tensile property of annealed Ti-6Al-4V under high magnetic field

Fig.2 presents the stress-displacement curves of the as built and the annealed SLM Ti-6Al-4V. The ductility/elongation of the annealed specimens are significantly enhanced when comparing with those of the as-built state, agreeing well with previous observations that the heat treatments improve the ductility of AM Ti-6Al-4V[17,19,21]. Besides the SLM-d specimen annealed at 800 °C, the ultimate tensile strength of SLM-a and SLM-e annealed specimens at 400 and 1200 °C were improved due to the short annealing time (30 min) when comparing with those of as-built ones. Although data scatter of tensile properties is also captured in our work, the purpose of the selected best results presented here is to highlight the variation tendency caused by the efficient magnetic-field-driving heat treatments. It is worth mentioning that the Aerospace Materials Specification SAE AMS4999A covers Titanium Alloy Direct Products Ti-6Al-4V Annealed, which suggests a post build annealed at 550 °C for the normal cases and in a temperature range of 899~954 °C together with stress no less than 100 MPa for 2 h followed by a slow cooling to below 427 °C during the HIP treatment[5]. In line with the ASM heat treatment handbook, annealing treatment in the temperature range of 705~790 °C for 1~4 h is recommended for Ti-6Al-4V in order to improve the ductility at room temperature, the fracture toughness, the creep resistance, and so on[45]. It has been reported that heat treatment at 500 °C for 10 h could relieve only 50% of the residual stresses[46].

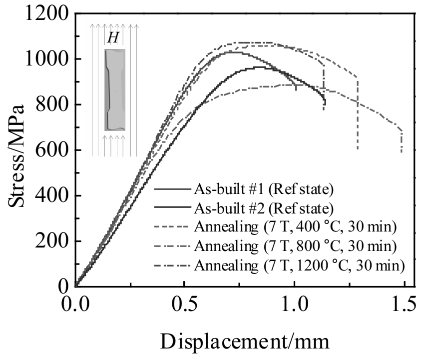

Fig.2 Stress-displacement curves of the as-built and the annealed specimens (the insert schematic diagram presents that the scanning direction of the SLM-processed specimen is parallel to the high magnetic field during annealing)

A residence time of approximately 8 h was required to achive 50% globularization of the α phase at 955 °C[17]. Therefore, the present results indicate that magnetic-field-driving heat treatments could efficiently optimize the mechanical properties of SLM Ti-6Al-4V.

2.2 Microstructures

In order to address the aforementioned major remaining challenge in improving the required minimum threshold ductility for critical structural applications, the decomposition/transformation of acicular α' martensite plays a dominate role. The transformation of acicular α' martensite into lamellar α+β is thermally activated and diffusion-controlled[12,47,48], when the SLM specimens are annealed at 400, 800 °C below the β transus, and 1200 °C above the β transus for 30 min in the high magnetic field of 7 T. Fig.3 shows the X-ray diffraction patterns of the as-built and the annealed specimens. It is found that the characteristic peaks associated with the α, β, and Ti_3Al phases agree well with previous observations[16,19,45,49,50]. The intensity of β phase peaks within the low angle range (<45°) seems to be increased after annealing at 1200 °C, indicating the associated $\alpha\rightarrow\beta$ transformations. On the contrary, the

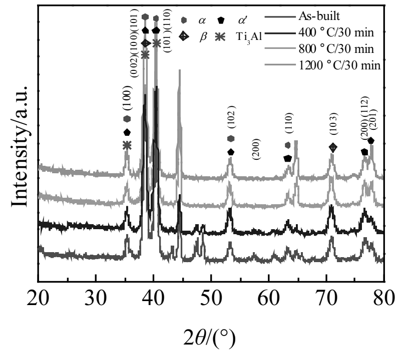

Fig.3 XRD patterns of the as-built and the annealed specimens at 400, 800 and 1200 °C under 7 T high magnetic field for 30 min

intensity of these peaks (<40°) seems to be reduced after annealing at 400 and 800 °C, which should correspond to $\beta\rightarrow\alpha$ transformations. It is understood that the grain refinement and the microdistortion contribute to the broadening of diffraction peaks[50], the latter of which could be considered as an indicator characterizing the lattice distortion minimization. According to the thermodynamic assessment of Ti-Al-V at 500, 800 and 1200 °C[51], it can be seen that the Ti_3Al phase formed during the processing with such a high temperature gradient can be removed by heat treatment. Moreover, there are also some abnormal peaks which haven't been reported, such as these peaks within the 40°~50° range. Since there is a long storage time for these specimens (several months), their surface could be rich in oxygen, which diffuse as the predominant phase along with a small amount of α and α/β peaks[52]. That is the reason why those peaks with low intensities are removed at high temperature.

Fig.4 and Fig.5 display the morphologies of grains of the SLM Ti-6Al-4V samples on the *XY* and the *YZ* planes, respectively. The yellow arrow in Fig.4 highlights the scanning direction of SLM process. The microstructures of the as-built SLM Ti-6Al-4V consist of acicular α' martensite and prior near-cellular β grains, matching well with the XRD results and previous observations[3]. It has been semi-quantitatively predicted that the majority of β laths form as a result of decomposition of α' martensite in a temperature range of 600~850 °C[16]. The transformation may be incomplete at insufficiently low temperature well below 500 °C, which will be finished already at 700~800 °C after 30 min tempering[26]. At the furnace and air cooling, β phase transforms to the acicular α-Widmanstatten structure by diffusional mechanism, while water quenching yields the formation of metastable hexagonal (M_s=800 °C) α martensite and some residual at grain boundaries[26]. Thus, the low-temperature (400 and 800 °C) and the high-temperature (1200 °C) annealing strategies are used to optimize the amount of β phase via controlling α' martensite of the SLM Ti-6Al-4V, shown in Fig.4b-1~4b-3, 4c-1~4c-3, and Fig.5b, 5c. The bright lines on the *YZ* planes correspond to the layer boundaries caused by the remelting during the SLM processing. It is noted that the width of these bright lines is about 100 μm, close to the size of the laser spot. Since the ultrafine lamellar $\alpha+\beta$ dual-phase structure in the SLM Ti-6Al-4V specimens results in not only a high yield strength but also a large elongation[19], the fine lamellar dual-phase structure is expected to be obtained. It can be seen that dark bands consisting of β phase become more obvious when increasing the annealing temperature from 400 °C to 800 °C, which are removed after a high temperature annealing.

Fig.6 shows the scanning electronic microscope images of the annealed SLM Ti-6Al-4V at 400 and 800 °C. It is clearly presented that the decomposition of α' martensite into α and β phases results in those fine lamellar features (~ 200 nm in thickness), which is similar to those images annealed at 400 °C for 2 h by Xu et al[19]. After annealing at 800 °C for 30 min, the grain size is larger than that at 400 °C, resulting in the

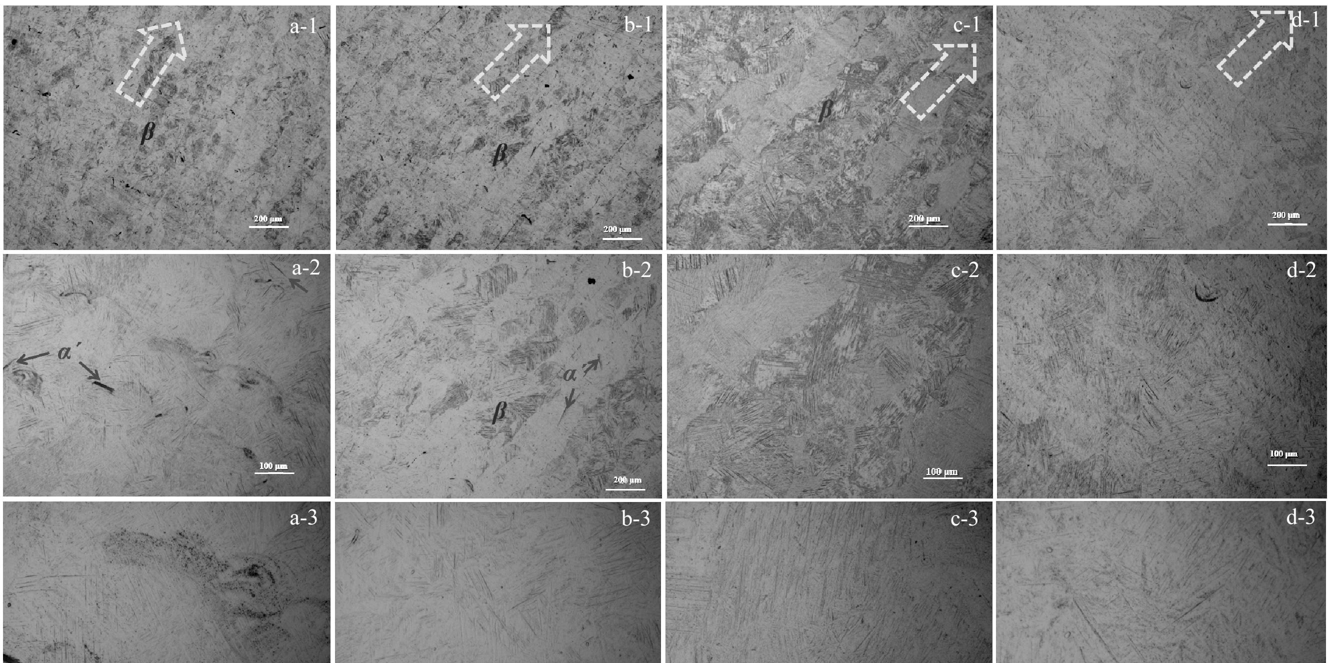

Fig.4 Optical morphologies of the SLM Ti-6Al-4V samples on *XY* plane: (a-1~a-3) the as-built samples; the samples annealed at 400 °C (b-1~b-3), 800 °C (c-1~c-3) and 1200 °C (d-1~d-3) under 7 T high magnetic field for 30 min

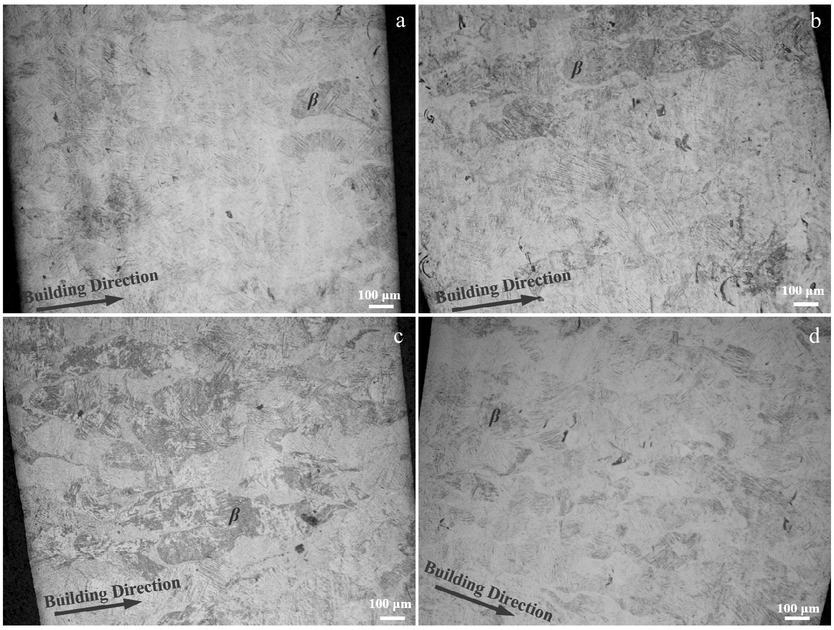

Fig.5 Optical morphologies of the SLM Ti-6Al-4V samples on *YZ* plane: (a) the as-built sample; the sample annealed at 400 °C (b), 800 °C (c) and 1200 °C (d) under 7 T high magnetic field for 30 min

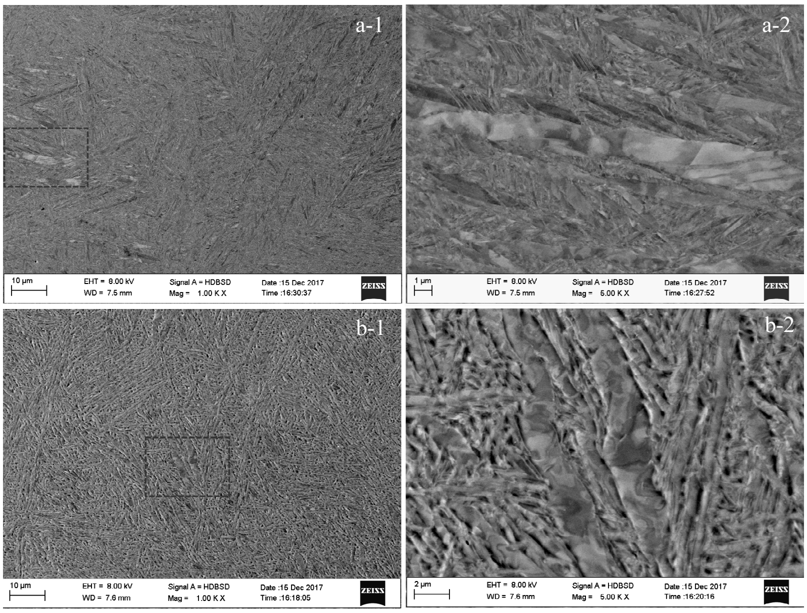

Fig.6 SEM images of the SLM-processed Ti-6Al-4V samples on *YZ* plane annealed at 400 °C (a-1, a-2) and 800 °C (b-1, b-2)

decreased tensile strength as shown in Fig.2. Moreover, the newly formed nano β particles could also disperse along the α boundaries[19], which are characterized as those high isolated point zones on the etched surface as shown in Fig.7. It has been reported that the V-containing α Ti-6Al-4V forms ordered cluster faster than the Ti-7Al[53]. Being a β phase stabilizer, V atoms would prefer to partition to the β phase during the decomposition of α' martensite, while Al atoms tend to segregate to the α phase, contributing to the formation of Ti_3Al compound[22]. Accordingly, as shown in Fig.7, the α and the β phases are rich in Al and V, respectively[19], yielding the difference in chemical potential and corrosion resistance responding to the acid etching and forming those stripes/ridges.

Fig.8 highlights the pores (dash circles) and the unmelt powder particles (solid circles) in the SLM Ti-6Al-4V, which have not been removed by the annealing. Those non-processed particles could act as nuclei for cracks[18]. In general, the porosity of AM Ti-6Al-4V can be reduced from 0.29% to

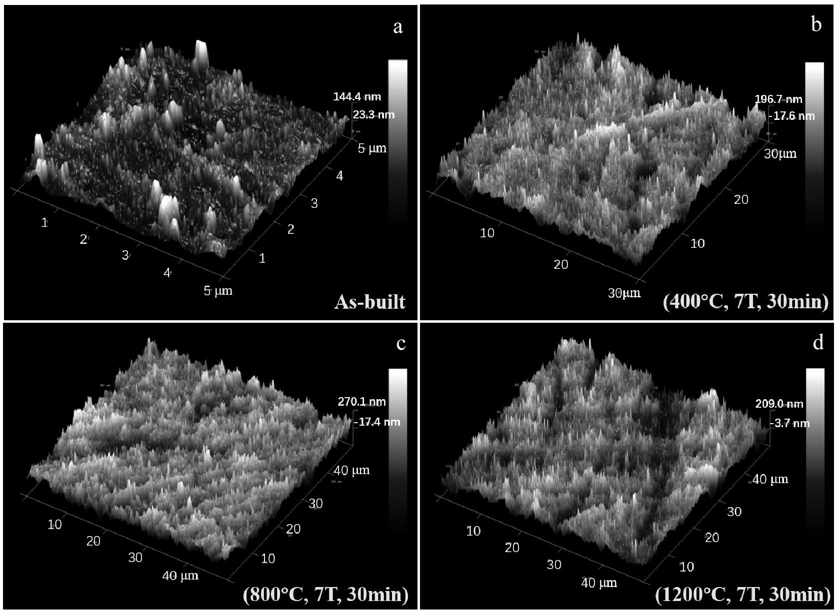

Fig.7 AFM images of the etched surface of the SLM-processed Ti-6Al-4V samples used for SEM: (a) the as-built sample; the samples annealed at 400 °C (b), 800 °C (c) and 1200 °C (d)

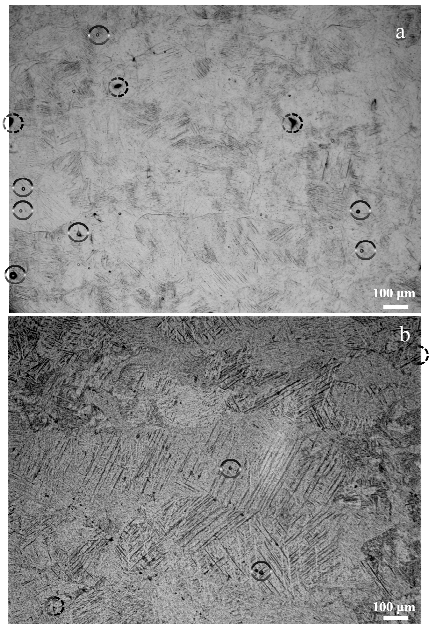

Fig.8 Optical morphologies of defects in the SLM Ti-6Al-4V samples on *YZ* plane annealed at 400 °C (a) and 800 °C (b)

0.074% through reinterring some poorly bound particles during the annealing[45]. Although the post-annealing treatment can reduce porosity by as high as 75%, the remaining pores still play an important role in reducing the mechanical properties[45], requiring a further treatment to modify/control those defects.

2.3 Lattice distortion induced phase transformations

Lattice distortion induced by Al and V atoms is characterized by bonding charge density, providing an insight into the atomic and electronic basis for the solid solution strengthening mechanism and the martensitic transformation mechanism, as shown in Fig.9. It can be seen that there are rod-type bonds in the α-$Ti_{95}X$ (X=Al, V, Mo), agreeing well with previous observations[37,42,54].

On the contrary, the chemical bond morphologies of the β-$Ti_{95}X$ are extremely complex, presenting wreath-type bonds. The enhanced bonding charge density indicates an improved bond strength[54]. On the one hand, the valence electron redistribution constructing these chemical bonds would not only reveal the solid solution strengthening mechanism but also provide an insight into the phase transformation path way. As shown in Fig.9, the bonding strength of Ti-Mo is significantly improved since there is a dense $\Delta\rho$. That is the reason why the molybdenum equivalency ($[Mo]_{eq}$)[55] is always considered as a kind of principles/criteria designing the advanced titanium alloys, providing an insight into the solid solution mechanism. Since the Al atoms reduce the d-electron concentration by two and the V atoms increase it by one, the Al atoms have a larger effect on the phase transformation pathway, i.e., $\alpha\rightarrow\omega$ transformation[56]. Due to the different atomic sizes, the substitution of Ti by Al and V will cause a local lattice distortion, which further modifies the phase transformation pathway. For example, due to the lattice distortion induced by the solid solution hydrogen and hydrides, the formation of orthorhombic α'' martensite and β phase have been captured in the hydrogenated Ti-6Al-4V alloys during water quenching, which further yield internal stress to promote the formation of α'' martensite and twins inside[57].

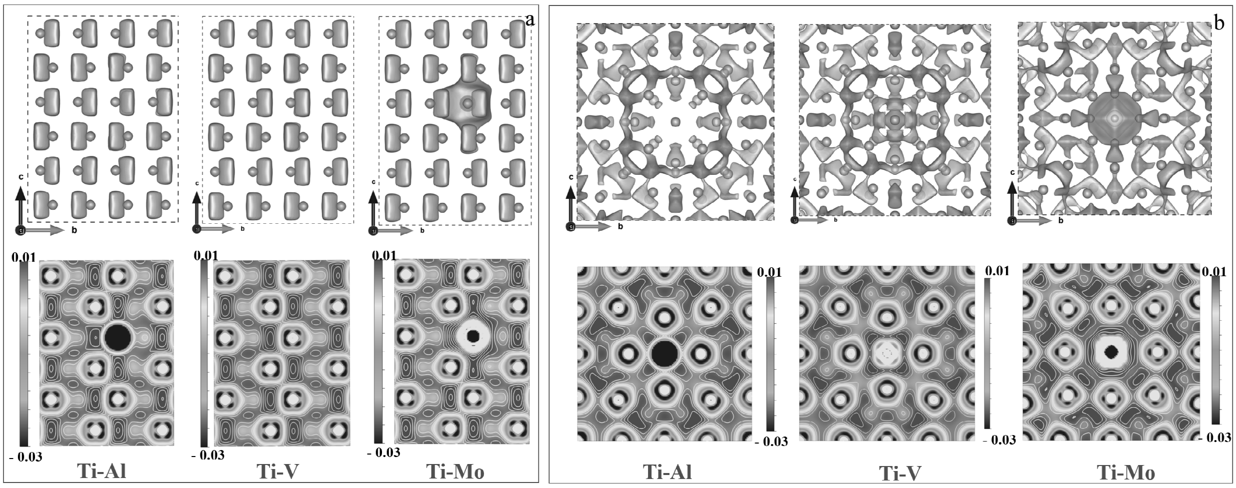

Fig.9 Effect of substitutional atoms on the bonding morphology of Ti characterized by bonding charge density isosurface and contour plots: (a) the α-$Ti_{95}X$ and (b) the β-$Ti_{95}X$

On the other hand, lattice distortion could result in anomalous ferromagnetism[58]. With the coupling effect of heat and high magnetic field, the phase transformation thermodynamics (i.e., driving force $\Delta G_{Total} = \Delta G_{Chem} + \Delta G_{mag}$) would become one type of novel phenomena to be further investigated, which is also the foundation of the present magnetic-field-driving approach efficiently to improve the mechanical properties of selective laser melting Ti-6Al-4V.

3 Conclusions

1) The ultimate tensile strength and the elongation of annealed SLM-Ti-6Al-4V at 400 and 1200 °C in 7 T high magnetic field increase due to the short annealing time.

2) The valence electron redistribution constructing these chemical bonds would not only reveal the solid solution strengthening mechanism but also provide an insight into the phase transformation path way. Since the Al atoms reduce the d-electron concentration by two and the V atoms increase it by one, the Al atoms have a larger effect on the phase transformation pathway.

3) Lattice distortion could result in anomalous ferromagnetism. Based on the coupling effect of force field induced by the heat and magnetic, the phase transformation thermodynamics would become one type of new phenomena to be further investigated. The validation of our proposed approach paves a path to develop a novel magnetic-field-driving approach efficiently to enhance the mechanical properties of additive manufactured materials.

References

1 DebRoy T, Wei H L, Zuback J S *et al*. *Progress in Materials Science*[J], 2018, 92: 112
2 Carroll B E, Palmer T A, Beese A M. *Acta Materialia*[J], 2015, 87: 309
3 He B B, Wu W H, Zhang L *et al*. *Vacuum*[J], 2018, 150: 79
4 Liu Y, Zhang J, Li S J *et al*. *Acta Metallurgica Sinica*[J], 2017, 30(12): 1163
5 Dutta B, Froes F H. *Metal Powder Report*[J], 2017, 72(2): 96
6 Pollock T M, Allison J E, Backman D G *et al*. *Integrated Computational Materials Engineering*[M]. Washington, DC: The National Academies Press, 2008
7 Pollock T M. *Nature Materials*[J], 2016, 15: 809
8 Shapira P. *Science*[J], 2017, 358(6366): 1007
9 Zhou J, Li P, Zhou Y *et al*. *Engineering*[J], 2018, 11: 20
10 Zhou J. *China Mechanical Engineering*[J], 2015, 26(17): 2273 (in Chinese)
11 Bobbio L D, Otis R A, Borgonia J P *et al*. *Acta Materialia*[J], 2017, 127: 133
12 Wu M W, Chen J K, Lin B H *et al*. *Materials & Design*[J], 2017, 134: 163
13 Bartolomeu F, Sampaio M, Carvalho O *et al*. *Journal of the Mechanical Behavior of Biomedical Materials*[J], 2017, 69: 128
14 Keist J S, Palmer T A. *Materials & Design*[J], 2016, 106: 482
15 Krakhmalev P, Fredriksson G, Yadroitsava I *et al*. *Physics Procedia*[J], 2016, 83: 778
16 Xu W, Lui E W, Pateras A *et al*. *Acta Materialia*[J], 2017, 125: 390
17 Vrancken B, Thijs L, Kruth J P *et al*. *Journal of Alloys and Compounds*[J], 2012, 541: 177
18 Kasperovich G, Hausmann J. *Journal of Materials Processing Technology*[J], 2015, 220: 202
19 Xu W, Brandt M, Sun S *et al*. *Acta Materialia*[J], 2015, 85: 74
20 Chern A H, Nandwana P, Yuan T *et al*. *International Journal of Fatigue*[J], 2018, 119: 173
21 Kok Y, Tan X P, Wang P *et al*. *Materials & Design*[J], 2018, 139: 565
22 Thijs L, Verhaeghe F, Craeghs T *et al*. *Acta Materialia*[J], 2010, 58(9): 3303
23 Yang J, Yu H, Yin J *et al*. *Materials & Design*[J], 2016, 108: 308
24 Leuders S, Thöne M, Riemer A *et al*. *International Journal of Fatigue*[J], 2013, 48: 300

25 Fatemi A, Molaei R, Sharifimehr S *et al*. *International Journal of Fatigue*[J], 2017, 100: 347
26 Yadroitsev I, Krakhmalev P, Yadroitsava I. *Journal of Alloys and Compounds*[J], 2014, 583: 404
27 Van Hooreweder B, Apers Y, Lietaert K *et al*. *Acta Biomaterialia*[J], 2017, 47: 193
28 Mukherjee T, Zhang W, DebRoy T. *Computational Materials Science*[J], 2017, 126: 360
29 Wauthle R, Vrancken B, Beynaerts B *et al*. *Additive Manufacturing*[J], 2015, 5: 77
30 Li P, Warner D H, Fatemi A *et al*. *International Journal of Fatigue*[J], 2016, 85: 130
31 Zhao X L, Li S J, Zhang M *et al*. *Materials & Design*[J], 2016, 95: 21
32 Gunther J, Krewerth D, Lippmann T *et al*. *International Journal of Fatigue*[J], 2017, 94: 236
33 Liu Z G, Wong T I, Huang W *et al*. *Acta Metallurgica Sinica*[J], 2017, 30(7): 630
34 Garcin T, Rivoirard S, Elgoyhen C *et al*. *Acta Materialia*[J], 2010, 58(6): 2026
35 Ohtsuka H. *Current Opinion in Solid State and Materials Science*[J], 2004, 8(3-4): 279
36 Peplow M. *Nature*[J], 2017, 544(7651): 408
37 Wang W Y, Zhang Y, Li J S *et al*. *Journal of Materials Science*[J], 2018, 53(10): 7493
38 Wang W Y, Xue F, Zhang Y *et al*. *Acta Materialia*[J], 2018, 145: 30
39 Wang W Y, Shang S L, Wang Y *et al*. *Npj Computational Materials*[J], 2017, 3: 23
40 Wang Y L, Kang Y L, Wang W Y *et al*. *Nanotechnology*[J], 2018, 29(41): 414 001
41 Kim H, Wang W Y, Shang S L *et al*. *Intermetallics*[J], 2018, 98: 18
42 Zou C X, Li J S, Wang W Y *et al*. *Computational Materials Science*[J], 2018, 152: 169
43 Nakashima P N H, Smith A E, Etheridge J *et al*. *Science*[J], 2011, 331(6024): 1583
44 Momma K, Izumi F. *Journal of Applied Crystallography*[J], 2011, 44: 1272
45 Xu Y Z, Lu Y, Sundberg K L *et al*. *Journal of Materials Engineering and Performance*[J], 2017, 26(6): 2572
46 Vilaro T, Colin C, Bartout J D. *Metallurgical and Materials Transactions A*[J], 2011, 42(10): 3190
47 Qazi J I, Senkov O N, Rahim J *et al*. *Materials Science and Engineering A*[J], 2003, 359(1-2): 137
48 Mur F X G, Rodriguez D, Planell J A. *Journal of Alloys and Compounds*[J], 1996, 234(2): 287
49 Xia J Y, Chai L J, Wu H *et al*. *Acta Metallurgica Sinica*[J], 2018, 31(11): 1215
50 Sun J F, Yang Y Q, Wang D. *Optics & Laser Technology*[J], 2013, 49: 118
51 Lindahl B, Liu X L, Liu Z K *et al*. *Calphad*[J], 2015, 51: 75
52 Kumar S, Narayanan T S N S, Raman S G S *et al*. *Materials Chemistry and Physics*[J], 2010, 119(1-2): 337
53 Radecka A, Bagot P A J, Martin T L *et al*. *Acta Materialia*[J], 2016, 112: 141
54 Wang W Y, Wang Y, Shang S L *et al*. *Materials Research Letters*[J], 2017, 5(6): 415
55 Fan J K, Kou H C, Zhang Y D *et al*. *Journal of Alloys and Compounds*[J], 2019, 770: 183
56 Hennig R G, Trinkle D R, Bouchet J *et al*. *Nature Materials*[J], 2005, 4: 129
57 Sun Z G, Chen G Q, Fu X S *et al*. *Acta Metallurgica Sinica*[J], 2010, 23(5): 357
58 Wang W Y, Shang S L, Wang Y *et al*. *Materials Chemistry and Physics*[J], 2015, 162: 748

强磁场下退火提高增材制造 Ti-6Al-4V 合金力学性能的研究

赵瑞峰[1]，李金山[1]，张　颖[1]，李佩璇[1]，王嘉祥[1]，邹程雄[1]，唐　斌[1]，
寇宏超[1]，甘　斌[1]，张　亮[2,3]，王　军[1]，王　毅[1]

(1. 西北工业大学 凝固技术国家重点实验室，陕西 西安 710072)

(2. 上海 3D 打印材料工程研究中心，上海 200437)

(3. 上海材料研究所，上海 200437)

摘　要：基于提出的一种崭新的磁场驱动方法有效地提高了激光选区熔化 Ti-6Al-4V 合金的力学性能。通过 X 射线衍射、光学显微镜、扫描电子显微镜和原子力显微镜，系统地表征了初始态和在 7 T 强磁场下退火 30 min 的样品的微观结构。其中，退火温度分别选取在低于 β 转变温度的 400 和 800 ℃，以及高于 β 转变温度的 1200 ℃。键合电荷密度不仅可以表征由 Al 和 V 原子引起的晶格畸变，还可以从电子和原子本质上揭示固溶强化机制和马氏体相变机制。由于退火时间较短，经 7 T 强磁场 400 和 1200 ℃退火的试样的极限抗拉强度和伸长率均比初始态的试样有所提高。上述结果表明，通过热和磁场的耦合效应，可以预期改变激光选区熔化 Ti-6Al-4V 合金的相变热力学，进而有效地优化其微观结构。这一设想的验证将有助于开发一种有效提高增材制造材料的力学性能的新型磁场驱动方法。

关键词：Ti-6Al-4V；激光选区熔化；热处理；键合电子密度

作者简介：赵瑞峰，男，1976 年生，研究员，西北工业大学凝固技术国家重点实验室，陕西 西安 710072，E-mail: 18618288307@139.com